JOURNAL OF MATERIALS SCIENCE 21 (1986) 1349–1356

Static mechanical properties of cast and sinter-annealed cobalt–chromium surgical implants

T. KILNER
Ryerson Polytechnical Institute, 350 Victoria Street, Toronto, Ontario M5B 2K3, Canada

W. M. LAANEMÄE*, R. PILLIAR, G. C. WEATHERLY
Department of Metallurgy and Materials Science, University of Toronto, Toronto M5S 1A4, Canada

S. R. MacEWEN
Materials Science Branch, Chalk River Nuclear Laboratory, AECL., Chalk River, Ontario K0J 1J0, Canada

Porous-surface-layered surgical implants may be produced by sintering at elevated temperatures. An investigation was undertaken to determine the effect of these sintering heat treatments on the tensile properties of the cobalt–chromium casting alloy specified by ASTM F75–76. Specimens which were given a sintering treatment and then rapidly cooled from elevated temperature were found to lack ductility. This was due to the incipient melting of an interdendritic material which was subsequently retained in the grain boundaries as a brittle solid after quenching. Two methods were found which would reduce the amount of this brittle solid: (i) modify the heat treatment to include a slow cooling step to temperatures below that at which incipient melting first occurred; and (ii) reduce the carbon content of the alloy. Reduced-carbon alloys gave the greatest post-sintering ductility, but showed a lower 0.2% yield stress. The techniques of thermal activation analysis were used to investigate the effect of second phases upon the initial low-strain work-hardening rates and the 0.2% yield stress. It was found that the work-hardening rate from the elastic limit to a total strain of about 0.01 to 0.02 depends, in part, directly on the volume fraction of second phase.

1. Introduction

Porous-surface-layered surgical implants are being studied extensively as an alternative to cemented and friction-held implants in orthopaedics and other disciplines. The rationale for their use is based upon the phenomenon of tissue ingrowth into the minute surface voids present on the prosthesis, thereby achieving mechanical fixation. Load-bearing implants such as the femoral component of porous-coated hip replacements are stabilized by the ingrowth of bone [1], and heart pacer electrode tips can be fixed to the endocardial tissue by soft tissue ingrowth, thereby limiting the extent of fibrous tissue formation at the electrode tip–myocardium interface, preventing scarring and consequent increases in electrical impedance in the pacemaker circuit [2]. Other applications are currently under clinical trial in the field of dentistry.

A convenient method of producing a porous surface layer on a solid metal implant is to coat the device with a metallic powder (normally of the same composition as the substrate), and then sinter the powder particles to each other and the substrate by heat treatment at temperatures close to the melting point of the alloy. Due to the metallurgical changes that take place during this process, such as recrystallization and grain growth, forged products are of little advantage as a substrate material. For this reason, one of the most common alloys used for the production of porous-surface-layered surgical implants is the cobalt–chromium casting alloy described by ASTM specification F75–76 (Table I). Typical carbon contents in finished products lie in the range 0.25 to 0.35 % wt, to ensure good strength and castability.

The mechanical properties of load-bearing implants are of concern, particularly in view of reported fatigue failures, well after implantation, of the stem components of hip prostheses [3]. As part of a programme directed towards the improvement of the mechanical properties of a variety of porous-coated implant materials, the static mechanical properties of F75–76 have been measured as a function of both carbon content and post-casting heat treatment. Of particular interest was the effect of the sintering step on tensile properties.

Present address: Max-Planck-Institut für Metallforshung, Institut für Werkstoffwissenschaften, Seestrasse 92, 7000 Stuttgart 1, West Germany.

0022–2461/86 $03.00 + .12

TABLE I ASTM F75–76 chemical requirements

Element	Minimum content (wt %)	Maximum content (wt %)
Chromium	27.0	30.0
Molybdenum	5.0	7.0
Nickel	–	2.5
Iron	–	0.75
Carbon	–	0.35
Silicon	–	1.00
Manganese	–	1.00
Cobalt	balance	balance

1.1. Metallurgical background

The usual heat treatment for cast cobalt–chromium–molybdenum implant alloys consists of a solution treatment at temperatures around 1473 K, for periods of about 1 h. The purpose of this treatment is to dissolve the interdendritic material remaining after casting, and to homogenize the microstructure. It results in improved static tensile properties, primarily increased ductility, over those found in the as-cast alloy.

Many investigators have studied different processing routes for improving the mechanical properties of the F75–76 type alloys. Weeton and Signorelli [4] found that a solution treatment followed by an ageing treatment at lower temperature increased the hardness of the alloy; no tensile data were reported. Asgar and Allen [5] measured the as-cast properties of F75 type alloys with a variety of alloying additions which were outside the standard ASTM specification. Hollander and Wulff [6] demonstrated that a hot isostatic pressing treatment (HIP) of cast F75–76, solution treated and aged at 923 K, resulted in static tensile property increases due to the healing of microvoids, compared to material that was solution treated and aged without a hot isostatic pressing. Ageing for 20 h of solution-treated material (not subjected to HIP) at 923 K, resulted in slight increases in tensile properties. Considerable scatter in the values was evident, for both the conventionally treated and material after HIP.

Devine and Wulff [7] showed that the tensile and fatigue strengths of wrought and heat treated (2 h at 1373 K) F75 type alloys were greatly increased compared to as-cast alloys of the same composition.

Cohen *et al.* [8] outlined a heat treatment consisting of a 4 h soak at 1088 K, to increase the size and volume percentage of intragranular precipitates, followed by a soak at 1498 K to dissolve intergranular precipitates, and finally quenching to produce a high density of interlocking bands of stacking faults. This treatment resulted in improved static tensile properties, to a maximum of 27% elongation and 0.2% yield strength of about 600 MPa, compared to the ASTM F75–76 minimum requirements for the as-cast material of 8% elongation and 450 MPa yield strength.

Recently Dobbs and Robertson [9] used a solution treatment at 1513 K and ageing at 993 K to determine if the mechanical properties could be improved without a loss in corrosion resistance. Tensile, corrosion fatigue and corrosion tests were done, and it was found that a partial solution treatment gave the greatest improvement in corrosion fatigue behaviour. Ageing was found to cause embrittlement with a great loss in ductility. This loss in ductility has been noted by others such as Cox [10] who found the high-cycle fatigue resistance to be highest in the as-cast alloy, with an ageing treatment at 973 K giving an increased 0.2% yield strength compared to solution treated material, but lower ductility.

VanderSande *et al.* [11] studied the behaviour of F75 alloys (cast and wrought) after a solution treatment at 1503 K and ageing at 923 and 1023 K. They found the ageing treatment promoted formation of stacking faults and an h c p phase, with an $M_{23}C_6$ precipitate eventually forming in the h c p areas. Static mechanical testing showed that an increase in yield strength resulted after 20 h of ageing at 923 K in the as-cast material. However, there was considerable variation in the yield strength, ranging from 470 to 720 MPa for the same material, compared to 450 MPa for the as-cast material. The ductility reported was comparable to the as-cast alloy, being in the range of 8 to 12%.

Taylor and Waterhouse [12] found that the peak increase in strength properties after ageing occurred when the material was aged at temperatures about 923 K. They concluded that the brittleness associated with this type of treatment rendered the process commercially useless.

Others [13–16] have used electron microscopy to investigate the microstructural behaviour of stacking faults and twins produced either by ageing at 923 to 1073 K, or by room-temperature cold-working. No mechanical test data were reported.

The porous-coating process requires the use of higher temperatures than those used in solution treating (1473 K). For good sintering of the metal powder particles within reasonable times (1 to 3 h), sintering temperatures in the range 1553 to 1583 K must be used. The effect on the microstructures of the elevated-temperature sintering treatments used for fabricating the porous-coated implants has been investigated and reported previously [17, 18]. These studies showed that in the as-cast condition the alloy consists of a cored structure of cobalt-rich dendrites, with an interdendritic eutectic resulting from the last solute-rich liquid to solidify during casting. This eutectic was identified, using electron-optical techniques, as a mixture of $M_{23}C_6$, sigma phase, and an f c c cobalt-rich phase.

The chemical composition of the interdendritic material was shown to be related to a eutectic found in the Co–Cr–C phase diagrams reported in the literature [19, 20]. Thermal analysis and microstructural observations indicated a melting temperature of 1508 K for this eutectic. At the sinter-annealing temperature (about 1573 K) the interdendritic material melts, producing a liquid phase along the grain boundaries. Subsequent quenching results in the formation of brittle secondary phases, as this grain-boundary liquid solidifies (Fig. 1a), and a severe decrease in tensile ductility is observed. Typical properties for 0.33% carbon Co–Cr–Mo tensile

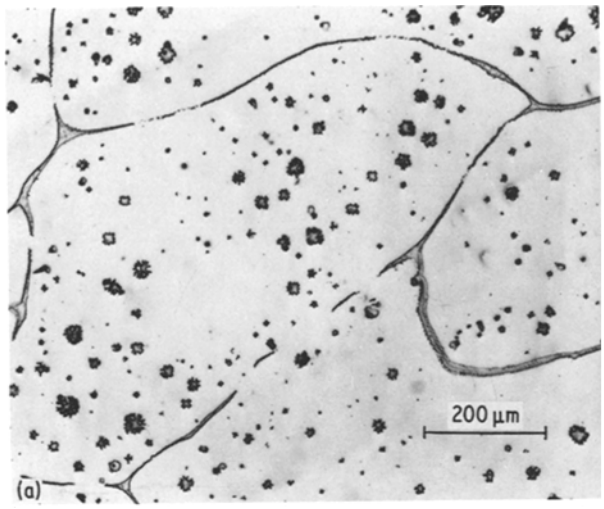

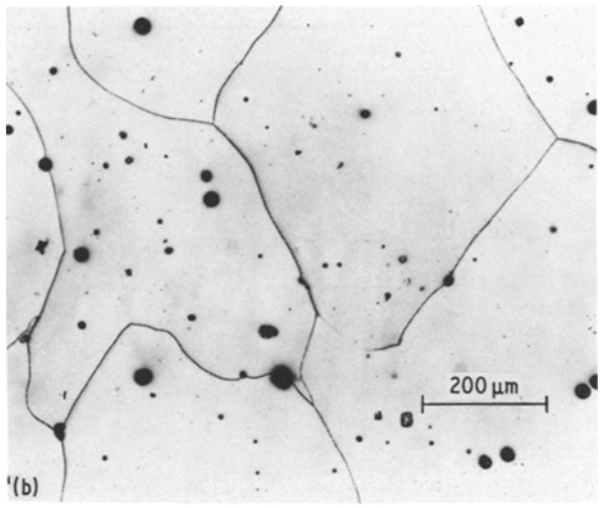

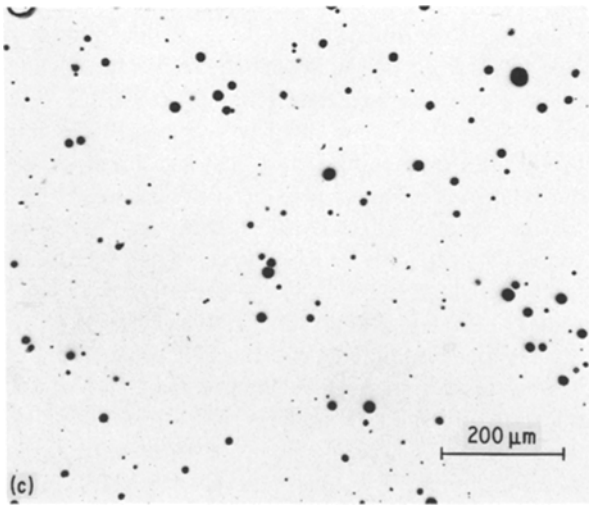

Figure 1 (a) Microstructure of 0.33% carbon tensile sample held at 1573 K for one hour, then water-quenched. Grain boundaries are outlined by brittle retained eutectic. (b) Microstructure of 0.33% carbon tensile sample held at 1573 K for one hour, then cooled at 2 K min^{-1} to 1493 K, held one hour, then water-quenched. Less second-phase material is present, both within grains and along grain boundaries. (c) Microstructure of 0.07% carbon tensile sample held at 1573 K for one hour, then water-quenched. Grain boundaries are free of carbides and resistant to etching using the same techniques as in (a) and (b). Extensive porosity is visible.

specimens (uncoated) that have been subjected to a typical sinter-annealing heat treatment (1573 K, 3 h, followed by rapid quenching) showed zero plastic elongation, 0.2% yield strength not measurable, and an ultimate tensile strength of about 480 MPa. The use of implants with mechanical properties such as these in load-bearing applications is not acceptable, and the development of a process that allowed sintering of a porous surface layer while avoiding the formation of the brittle grain-boundary phase after sintering was required.

1.2. Heat treatment and alloy modifications

Heat treatments designed to reduce or eliminate the grain-boundary phase were developed by us and reported in previous metallographic studies [17, 18]. They were based upon the principle of slowly cooling the sample after sintering, from the sintering temperature to a temperature just below the freezing point of the interdendritic eutectic (1508 K), and then quenching. Cooling rates in the slow cooling stage were of the order of 1 K min^{-1}. This low rate allowed the interdendritic liquid phase to approach equilibrium proportions with the matrix as the temperature approached the solidus, and resulted in greatly reduced amounts of solid eutectic in the grain boundaries (Fig. 1b). Rapid quenching from the sintering temperature retained a larger proportion of the grain-boundary liquid phase as a brittle solid at room temperature. (Compare Figs. 1a and b).

A second approach to the elimination of retained second phase at the grain boundary after sintering is to modify the alloy chemistry. Since the interdendritic eutectic is appreciably enriched in carbon [17], by lowering the carbon content of the alloy the amount of second phase which can form during sintering is also reduced. The series of alloys used in this study ranged in carbon content from 0.07 to 0.33 wt %. Heat treatment of these alloys, using simulated porous coating steps, showed that in the lowest carbon formulations (0.07% C), there was no retention of secondary grain-boundary phases regardless of the cooling rate used from 1573 K (Fig. 1c). Since brine quenching was often employed this would indicate that the alloy exists as a single phase at 1573 K, when carbon levels are at or below 0.07% C.

1.3. Thermal activation analysis

In the F75–76 alloy there are many possible strengthening mechanisms due to the complexity of the alloy. The number of solutes which can cause solute strengthening, the interaction of stacking faults, and the presence of second-phase particles in structures resulting from some heat treatments, can all contribute to strengthening, manifested by an increase in the flow stress.

The nature of the obstacles controlling dislocation motion and thus plastic flow can be determined using a thermal activation analysis. A characteristic of one of the activation events is the activation area, i.e. the area swept out past the obstacle by the dislocation on the glide plane during thermal activation. The true activation area cannot be readily measured; however, an apparent activation area, which also reflects the

TABLE II Chemical analyses of F75–76 alloys used*

Alloy	Content (wt %)								
	Mo	Cr	Mn	Fe	Co	Ni	Si	Ti	C
1	6.07	27.9	0.04	0.35	64.0	0.46	0.05	003	0.33
2	5.78	27.0	0.13	0.43	65.4	0.44	0.68	0.01	0.19
3	5.81	27.3	0.13	0.46	65.1	0.44	0.65	0.01	0.17
4	5.80	27.1	0.14	0.44	65.3	0.43	0.69	0.01	0.12
5	5.80	27.3	0.14	0.43	65.1	0.43	0.70	0.01	0.07
6	6.5	27.0	0.6	0.7	bal	0.6	1.5	0.03	0.25

*Alloys 1 to 5 were used for the standard tensile tests described in the text. Alloy No. 6 was used for the thermal activation analysis tests.

statistical distribution of obstacles in the structure, may be determined from

$$\Delta a' = \frac{kT}{b} \frac{\mathrm{d} \ln \dot{\varepsilon}}{\mathrm{d}\sigma}$$

where k is Boltzmann's constant, T the absolute temperature, b the Burgers vector of the dislocation, $\dot{\varepsilon}$ the strain rate and σ the stress [21–23]. $\mathrm{d} \ln \dot{\varepsilon}/\mathrm{d}\sigma$ can be found experimentally from either stress relaxation or strain-rate change tests.

As important as the activation area itself is its variation with flow stress. Both the activation area and the flow stress depend on the nature and density of the obstacles. In the case of a pure metal, dislocations are the only obstacles which can vary in density during straining. Work hardening increases the flow stress by increasing the dislocation density. The activation area similarly depends on the nature and distribution of the obstacles, and a plot of the reciprocal of activation area against the flow stress for different dislocation densities, first proposed by Cottrell and Stokes [24] but commonly known as a Haasen plot [25], would be a straight line through the origin.

In an alloy, the Haasen plot would show a positive intercept on the inverse activation-area axis if the obstacles to dislocation motion are solute atoms, and a negative intercept if the obstacles are particles of a second phase. It is thus possible using thermal activation analysis to determine the nature of the obstacles contributing to the flow stress, without recourse to other methods such as electron microscopy [22].

2. Experimental methods

Several cast Co–Cr–Mo–C alloys meeting the ASTM F75–76 specification were used in this study, with carbon contents ranging from 0.07 to 0.33% C (Table II). The standard tensile specimens were cast conforming to ASTM E8–69 specifications for standard threaded-end tensile specimens of 6.25 mm diameter. Other specimens intended for thermal activation analysis were machined to an overall length of 10.2 cm by 1.27 cm diameter, with a reduced-area region 2.54 cm long with a diameter of 0.635 cm. The tapered portion had a radius of curvature of 2.54 cm and blended smoothly into the reduced-area portion of the specimen.

The alloys were subjected to heat treatments that were intended to simulate the sintering of a powder-made porous surface coating to the cast substrate surface. As-cast and conventional solution-treated samples were also tested. The heat treatments were carried out in a high-temperature vacuum furnace at a pressure of 6×10^{-4} Pa, with microprocessor-controlled temperature programming, allowing experimentation with a wide variety of predetermined heating rates, dwell times and cooling rates. Quenching after heat treatment was done using high-purity helium directed at the specimen, resulting in quench rates of approximately 400 K min^{-1} at 1373 K. Specimens treated in this manner were typically clean and bright after quenching. After heat treatment the standard tensile test specimens were tested in air on an Instron mechanical testing machine at a crosshead speed of 2 mm min^{-1}. Four specimens for each different carbon content and heat treatment were usually tested.

Specimens intended for thermal activation analysis were tested using an MTS Alpha testing system under microprocessor control. Stress relaxation tests [21–23] were carried out on specimens that were as-cast, solution-annealed, solution-annealed for 40 h, sinter-annealed, and sinter-annealed–slow-cooled. The base strain rate was set to 10^{-3} sec^{-1} and stress relaxations were performed at increments of about 50 MPa at strains > 0.01. The specimens was allowed to relax for 15 to 30 min during each relaxation. The total strain was maintained constant throughout the relaxation period.

Specimens were prepared for metallographic examination using standard grinding and polishing techniques followed by electrolytic polishing in a solution of 90 vol % ethanol and 10 vol % perchloric acid at voltages of about 30 V and temperatures of about 10° C. Selected samples were also examined using scanning electron microscopy (SEM).

3. Results

Treatment Q in Table III shows the effect of a rapid quench from the sintering temperature on the tensile properties of the different alloys. There is a severe decrease in the ductility of the tensile samples as the carbon content increases, until at 0.33 wt %C the elongation to fracture becomes zero. At the lower carbon contents this effect is modified, and elongations approaching 20 % are observed; however, the 0.2 % yield strength shows a steady decrease as carbon content decreases.

Treatments S/C and P/C (Table III) show the effect of slow cooling to below 1508 K (the melting point reported for the eutectic [17]) on the properties of the alloys. Again, the percentage elongation to failure

TABLE III Tensile test results for different carbon contents (four samples tested in each category)

Alloy	Heat treatment	Elongation (%)	0.2% Yield stress (MPa)	UTS (MPa)
1 (0.33%C)	A/C*	2.7 to 3.8	570 to 590	740 to 760
	Q†	0	–	450 to 500
	S/C‡	4.9 to 9.4	540 to 550	680 to 760
	P/C§	5.0 to 6.7	490 to 500	630 to 640
2 (0.19%C)	A/C	5.3 to 5.7	530	750 to 760
	Q	2.5 to 8.4	500 to 520	590 to 720
	S/C	7.0 to 11.3	490 to 510	680 to 760
	P/C	6.0 to 9.4	460 to 470	610 to 660
3 (0.17%C)	A/C	7.8 to 8.0	500	760 to 770
	Q	2.7 to 11.1	420 to 500	470 to 730
	S/C	10.4 to 15.1	440 to 490	720 to 740
	P/C	9.7 to 14.8	410	590 to 650
4 (0.12%C)	A/C	6.5 to 7.1	500 to 520	680 to 710
	Q	17.3 to 19.7	430 to 450	720 to 750
	S/C	17.5 to 20.5	440 to 450	750 to 770
	P/C	13.4 to 15.6	390 to 400	620 to 640
5 (0.07%C)	A/C	4.2 to 5.5	510 to 520	650 to 660
	Q	14.5 to 16.1	410 to 420	640 to 680
	S/C	10.1 to 17.5	400	610 to 720
	P/C	19.6 to 20.3	360 to 370	660

*As-cast.
†Air atmosphere, 30 min heat up to 1573 K, 1.5 h at 1573 K, water quench.
‡Air atmosphere, 1 h heat up to 1573 K, 13 min at 1573 K, slow cool (2 K min^{-1}) to 1493 K, 9 min at 1493 K, water quench.
§Vacuum 15 min heat up to 1518 K, 10 min heat up to 1568, 60 min soak at 1568 K, slow cool (1 K min^{-1}) to 1473 K, 30 min soak at 1473 K, helium quench.

increases as carbon content decreases, and the 0.2% yield strength decreases as carbon decreases, ultimately ending up well below 400 MPa. However, the 0.33 % carbon alloy retains a high yield strength, while showing improved ductility over the quenched 0.33 % carbon samples, thereby suggesting the usefulness of this treatment for preparing porous-coated Co–Cr–Mo cast alloys.

Fig. 2a shows the results of tensile tests on Alloy No. 6 (0.25 wt %C) given the three heat treatments described below, using the MTS Alpha testing system:

1. Sinter-annealing at 1573 K for 2 h, followed by helium gas quenching.
2. Solution treatment at 1503 K for 1 h, followed by water quenching.
3. Slow cooling after sinter-annealing (1573 K for 2h, cooled at 1 K min^{-1} to 1474 K, held for 30 min followed by helium gas quenching).

Considerable differences in the work-hardening rate (i.e. the slope of the true stress–true strain curve at a given stress) for the three heat treatments may be seen from these curves for strains up to about 0.01 (Fig. 2b). After rapid work-hardening up to 0.01 strain, all the samples showed a low rate of work-hardening, ~1800 MPa at 0.05 strain, which was independent of the heat treatment given to the alloy.

Fig. 2c shows the Haasen plot for the above three heat treatments on the 0.25 % carbon alloys. There are no significant differences between the heat treatments. All the data shown in this plot were obtained after the initial rapid rate of work-hardening, i.e. at strains > 0.01. The resulting line was fitted by least-squares technique, and had a coefficient of correlation of 0.91. The intercept may be seen to lie on the positive inverse-activation-area axis, and was found to have a value of 0.76 with a standard deviation of 1.05.

4. Discussion

The simplest method of improving the ductility of porous-coated Co–Cr–Mo implants would be to use a low-carbon formulation, since this allows a simple one-stage heat treatment operation, with no need for a controlled cooling step. The resulting low yield strengths of the low-carbon alloys, however, are of concern particularly in view of the fact that the ASTM specification for the F75 alloy gives a minimum 0.2 % yield strength of 450 MPa, and ultimate strength of 655 MPa. A satisfactory combination of adequate ductility and yield strength can be obtained in the high-carbon alloys by slow-cooling after sintering.

The microstructural features that control the rate of work-hardening at high strains in the cobalt-based alloys have been discussed by Rajan [15] and Rajan and VanderSande [16]. They attributed the work-hardening to the low stacking fault energy of the alloy. Interactions between moving dislocations and the intersections of dissociated dislocations are the primary cause of work hardening. At very high strains, twinning and stress-induced transformations to the hcp phase become important. The present results show that an additional factor must be important in controlling the initial rate of work-hardening and the 0.2 % yield stress. We believe that this factor is related to the coarse carbides or second-phase particles.

A detailed examination of the stress–strain curves obtained with the MTS Alpha system (which permitted a high level of data acquisition at low strains

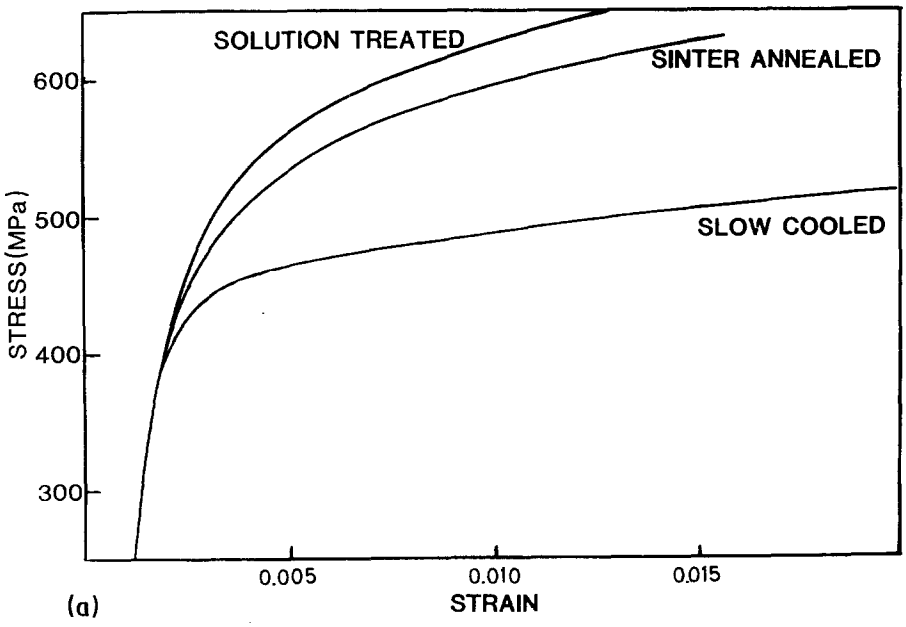

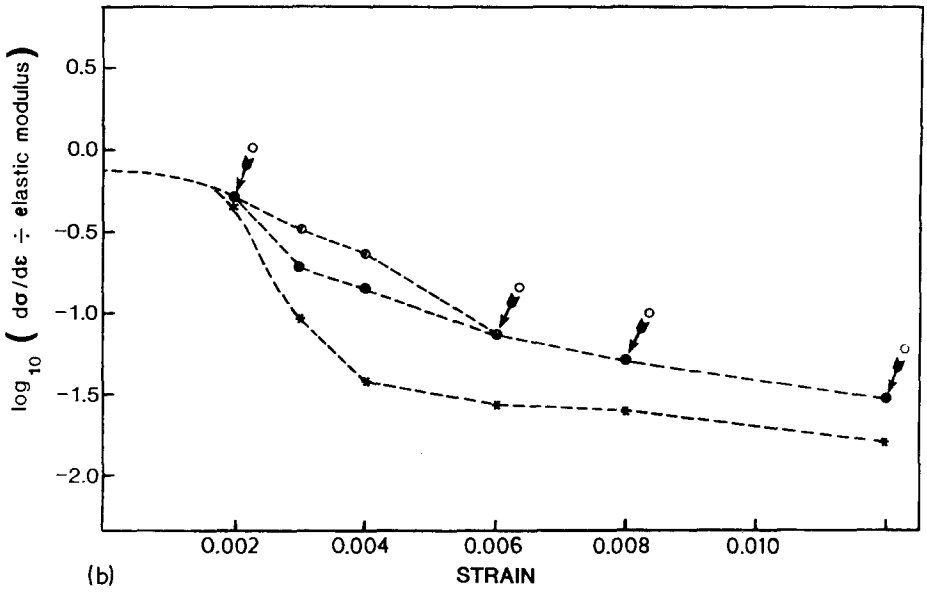

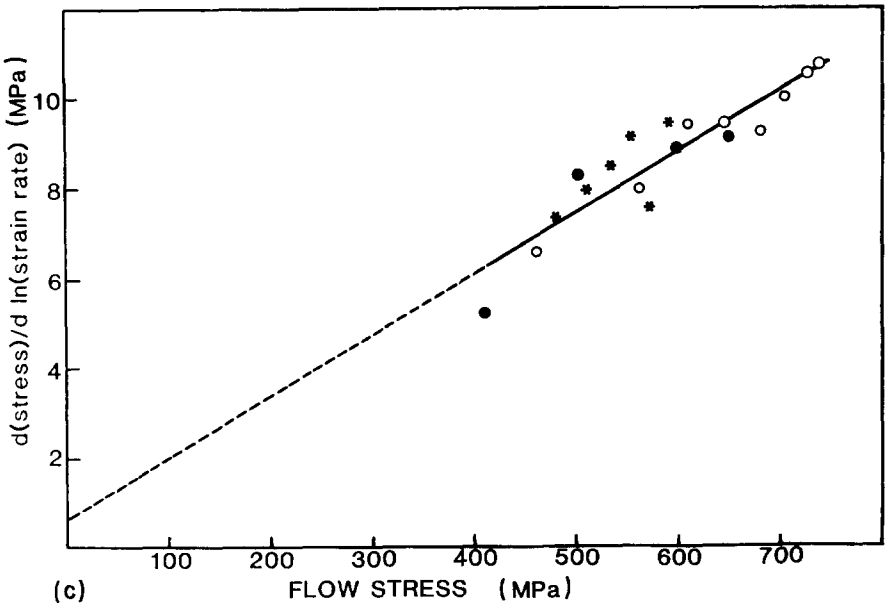

Figure 2 (a) Stress–strain curves for Alloy 6 (0.25 %C) given three different types of heat treatment; (b) work-hardening rates measured from the stress–strain curves shown in (a); (c) Haasen plot for Alloy 6 given three different types of heat treatment. (●) Sinter-annealed, (*) slow-cooled, (○) solution-treated.

(Fig. 2a)) shows that they may be divided into three distinct regions:

1. The elastic region which extends up to the proportional limit, which is ~ 300 MPa for all the heat treated alloys.
2. A region of rapid hardening, the rate of which varies with the volume fraction of second-phase particles (see below), from the proportional limit to a total strain of ~ 0.01 to 0.02.
3. A region of low work-hardening at strains greater than 0.02 which is independent of the heat treatment of the alloy.

The work-hardening rate in Region 2 is determined by two factors: (i) the transition from a fully elastic to fully plastic state as grains of different crystallographic orientation yield, and (ii) the distribution of coarse carbides or second-phase particles which act as elastic inclusions to reinforce the plastic matrix. The work-hardening rate associated with the latter effect depends on the volume fraction, shape and elastic modulus of the particles [26]. Provided the particles neither crack nor promote secondary slip, the rate of work-hardening is linear and is proportional to the volume fraction of the second phase [26].

We believe that this accounts for the observed differences with heat treatment shown by the stress–strain data in Fig. 2a. The volume fractions of second-phase particles for the three heat treatments of Alloy No. 6 were found to be ~ 0.05 (sinter-annealed), ~ 0.04 (solution-treated) and ~ 0.01 (sinter-annealed, slow-cooled). These figures are in accord with the trend shown by the data in Fig. 2a, i.e. the stress–strain curves for the solution-annealed and sinter-annealed samples are similar and show a much higher initial rate of work-hardening than the sinter-annealed and slow-cooled sample (Fig. 2b). The differences in the 0.2 % yield-stress values for the heat-treated samples can also be related to the initial work-hardening rate after the proportional limit. The distribution of coarse particles, although not normally considered beneficial to the mechanical properties of the alloys, is important in this context to help meet the ASTM specification of a minimum yield stress of 450 MPa.

The high rate of work-hardening that marks the initial portion of the stress–strain curves is confined to total strains of ~ 0.01 to 0.02. Beyond this strain value both the Haasen plot (Fig. 2c) and the low rate of work-hardening suggest that the flow stress is controlled either by dislocation–dislocation interactions or dislocation–solute interactions. The intercept made by the Haasen plot data was shown by statistical methods to be not significantly different from zero, suggesting that dislocation–dislocation interactions of the type considered by Rajan [15] determine the flow stress. The magnitudes of the activation areas found in this study were similar to those found by Mulford [22] for Inconel 600, which has a similar microstructure. The reinforcing effect of the coarse carbides is limited at strains > 0.02, probably because the carbides crack as the stress in the particles increases with increasing plastic strain. Evidence of extensive cracking of the carbide particles was obtained after deformation (see Fig. 3), and coarse particles such as these are expected to fracture at relatively low total plastic strains.

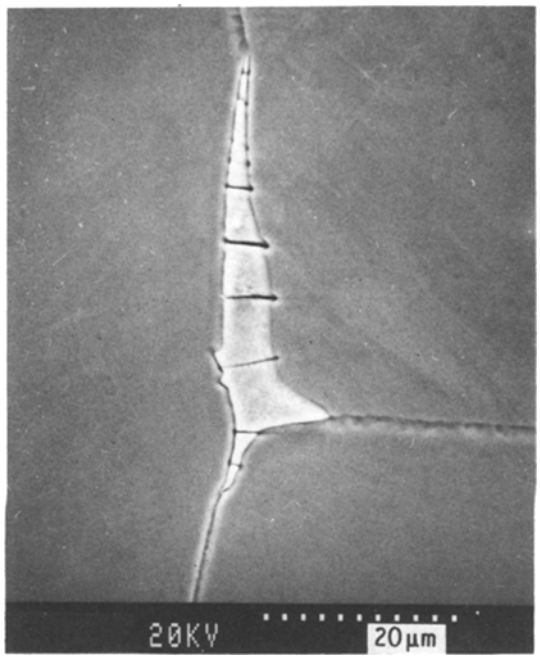

Figure 3 Cracked second-phase material appearing in a tensile test specimen after deformation.

5. Summary

A porous surface layer may be applied to surgical implants made from the F75–76 cobalt-based casting alloy by sintering, without adversely affecting the room-temperature ductility. This may be accomplished in one of two ways:

(i) by slowly cooling the part after sintering to temperatures below about 1500 K before quenching, or

(ii) by lowering the carbon content of the alloy. An adverse side effect of the lowered carbon content is an accompanying lowered 0.2 % yield stress of the alloy.

Thermal activation analysis illustrates the importance of the presence of second phases such as carbides for the work-hardening rate and the 0.2 % yield stress of the alloy. This effect will partially account for the reduced 0.2 % yield stress observed in low-carbon formulations of the alloy. A satisfactory combination of high yield stress and adequate ductility (i.e. a yield stress and percentage elongation comparable to the ASTM specification for the as-cast material) may be attained in the higher-carbon formulations of the alloy.

Adhering to the ASTM specifications for the high-carbon alloys brings with it problems such as coarse second phases, which can only be eliminated by resorting to more complex heat treatments. An alternative route to even greater ductility and higher yield stress at room temperature may lie in modifications to the lower carbon formulations, designed to increase the yield stress in an alloy with an already high ductility after sinter-annealing.

Acknowledgements

The authors would like to acknowledge the financial support of Canadian Oxygen Ltd and the Natural Sciences and Engineering Research Council of Canada. The technical assistance of J. Mecke and N. Christodoulou, Materials Science Branch, Chalk River Nuclear Laboratories, is appreciated.

References

1. R. M. PILLAR, *Clin. Orthop.* **176** (1983) 42.
2. J. D. BOBYN, G. J. WILSON, T. R. MYCIK, P. KLEMENT, G. A. TAIT, R. M. PILLAR and D. C. MACGREGOR, *PACE* **4** (1981) 405.
3. J. O. GALANTE, W. ROSTOKER and J. M. DOYLE, *J. Bone Joint Surg.* **57A** (1975) 230.
4. J. W. WEETON and R. A. SIGNORELLI, *Trans. ASM* **47** (1955) 815.
5. K. ASGAR and F. C. ALLEN, *J. Dent. Res.* (March/April 1968) 189.
6. R. HOLLANDER and J. WULFF, *Eng. Med.* **3** (4) (1974) 8.
7. T. M. DEVINE and J. WULFF, *J. Biomed. Mater. Res.* **9** (1975) 151.
8. J. COHEN, R. M. ROSE and J. WULFF, *ibid.* **12** (1978) 935.
9. H. S. DOBBS and J. L. M. ROBERTSON, *J. Mater. Sci.* **18** (1983) 391.
10. D. O. COX, PhD Thesis, University of California (1977).
11. J. B. VANDERSANDE, J. R. COKE and J. WULFF, *Met. Trans.* **7A** (1976) 389.
12. R. M. J. TAYLOR and R. B. WATERHOUSE, *J. Mater. Sci.* **18** (1983) 3265.
13. P. A. BEAVEN, P. R. SWANN and D. R. F. WEST, *ibid.* **13** (1978), 691.
14. *Idem, ibid.* **14** (1979) 354.
15. K. RAJAN, *Met. Trans.* **13A** (1982) 1161.
16. K. RAJAN and J. B. VANDERSANDE, *J. Mater. Sci.* **17** (1982) 769.
17. T. KILNER, R. M. PILLIAR, G. C. WEATHERLY and C. ALLIBERT, *J. Biomed. Mater. Res.* **16** (1982) 63.
18. T. KILNER, G. C. WEATHERLY and R. M. PILLIAR, *Scripta Metall.* **16** (1982) 741.
19. V. W. KÖSTER and F. SPERNER, *Arch. Eisenhuttenwesen* **26** (1955) 555.
20. P. R. SAHM, M. LORENZ, W. HUGI and V. FRUHAUF, *Met. Trans.* **3** (1972) 1022.
21. U. F. KOCKS, A. S. ARGON and M. F. ASHBY, *Prog. Mater. Sci.* **19** (1975).
22. R. A. MULFORD, *Acta Metall.* **27** (1979) 1115.
23. R. A. MULFORD and U. F. KOCKS, *ibid* **27** (1979) 1125.
24. A. H. COTTRELL and R. J. STOKES, *Proc. R. Soc.* **233A** (1955) 17.
25. P. HAASEN, in "Dislocations in Solids", edited by F. R. N. Nabarro (North Holland, Amsterdam, 1979) p. 155.
26. L. M. BROWN and D. R. CLARKE, *Acta Metall.* **23** (1975) 821.

Received 2 May
and accepted 12 June 1985